Insight into mechanisms of creatinine optical sensing using fluorescein-gold complex

Sara Anselmo[1], Giuseppe De Luca[2], Vittorio Ferrara[1], Bruno Pignataro[1], Giuseppe Sancataldo[1]* and Valeria Vetri[1]

[1]Dipartimento di Fisica e Chimica – Emilio Segré, Università degli Studi di Palermo, Viale delle Scienze ed. 18, 90128 Palermo, Italy
[2]Dipartimento di Scienze e Tecnologie Biologiche Chimiche e Farmaceutiche (STEBICEF), Università degli Studi di Palermo, Viale delle Scienze ed. 16, 90128 Palermo, Italy

*Corresponding author: giuseppe.sancataldo@unipa.it

Abstract

Creatinine level in biological fluids is a clinically relevant parameter to monitor vital functions and it is well assessed that measuring creatinine levels in the human body can be of great utility to evaluate renal, muscular, or thyroid dysfunctions. The accurate detection of creatinine levels may have a critical role in providing information on health status and represents a tool for the early diagnosis of severe pathologies. Among different methods for creatinine detection that have been introduced and that are evolving with increasing speed, fluorescence-based and colorimetric sensors represent one of the best alternatives, thanks to their affordability, sensitivity and easy readability.

In this work, we demonstrate that the fluorescein-Au^{3+} complex provides a rapid, selective, and sensitive tool for the quantification of creatinine concentrations in ranges typical of sweat and urine. UV-visible absorption, diffuse reflectance spectroscopy, steady state and time resolved fluorescence spectroscopy were used to shed light on the molecular mechanisms involved in the changes of optical properties, which underlie the multiplexed sensor analytical reply. Interestingly, sensing can be performed in solution or on solid nylon support accessing different physiological concentrations from micromolar to millimolar range. As a proof-of-concept, the nylon-based platform was used to demonstrate its effectiveness in creatinine detection on a solid and flexible substrate, showing its analytical colorimetric properties as an easy and disposable creatinine point-of-care test.

Graphical Abstract

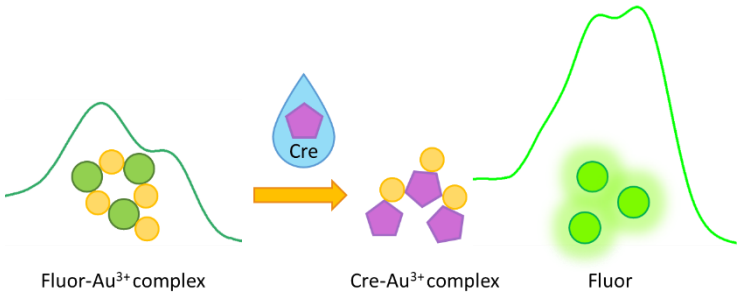

1. Introduction

The rapid and sensitive recognition of creatinine (Cre) is of great significance as it can represent a fundamental tool in clinical diagnosis of several pathologies[1,2]. Cre molecular concentration in serum, sweat and in urine outside the physiological ranges is evidence of health issues associated with renal and muscular functioning. The physiological concentration of Cre is 4.4 − 18 mM in urine, 45 – 90 µM in blood serum and 9.4 – 18 µM in sweat[2].

Nowadays, home-used fast medical tests are increasingly widespread and the development of easy and reliable point-of-care tools for fast determination of Cre in biological fluids (such as saliva, sweat, and urine) is highly relevant.

Traditional methods to detect Cre are based on the Jaffe's reaction, which exploits the colour change occurring upon the reaction of Cre with an alkaline solution of picrate[2]. Unfortunately, despite its cost-effectiveness and rapid analysis, this method is poorly selective and its sensitivity is affected by temperature and pH[2,3]. Due to the importance of revealing Cre molecule in biological fluids, several methods based on surface-enhanced Raman scattering (SERS)[4], liquid chromatography-isotope dilution mass spectrometry (LC-IDMS)[5], capillary electrophoresis[6], and electrochemistry have been developed aiming at providing more stable and selective methods. Some of these methods need laborious sample preparation steps, complex and environmentally toxic reagents, and the use of expensive and sophisticated instruments. In most cases, their use is not accessible to unspecialised users and only few expensive commercial kits are available[7–9]. Hence, a fast, simple, inexpensive, highly sensitive, and specific method to detect and quantify Cre is required. Among the most promising alternatives, optical sensors, such as fluorescence-based and colorimetric sensors, have received a great interest[10–15]. The ease of readability and signal transduction, together with the exquisite sensitivity and selectivity of fluorescence, are the main advantages. Examples of

fluorescence-based sensors used for Cre detection in aqueous solution are the Naphthalimide-lead[10] and Rhodamine B-gold[11] complexes. These complexes are not fluorescent but their dissociation, induced by Cre, and the consequential release of the free dyes (Naphtalimide and Rhodamine B) cause a turn on of the fluorescence that is quantified by means of intensity-based methods.

Colorimetric sensors based on silver[12] and gold[16,17] nanoparticles are also gaining growing attention due to their excellent sensitivity, inexpensiveness, and ease of detectability of different biologically relevant molecules, such as DNA, protein and organic compounds, including Cre[18]. Importantly, colorimetric detection represents a promising tool for commercial applications as the read out can be achieved by naked eye or commercial cameras like smartphone's[19].

In this work, we designed a simple and quick-response sensing platform, based on the complexation between fluorescein dye and gold ions (fluorescein-Au^{3+} complex), for the selective recognition of Cre in different concentration regimes.

Fluorescein is a water-soluble fluorescent dye, that thanks to its well-known properties, such as high quantum yield, sensitivity to the micro-environment and large availability, is widely used as tracer for many biological and medical applications[20–22]. It has also already been used in the field of sensing organic molecules, in complexed form with gold nanoparticles, as for the detection of the pesticide fenitrothion, potentially harmful for humans[23,24].

Here, we exploit the spectral changes in the optical range induced by the formation of fluorescein-Au^{3+} complex and its dissociation/modification following the interaction with Cre molecules for the quantification of this important biomarker both in the micromolar and millimolar concentration ranges. The molecular mechanisms involved in their interaction were investigated by means of UV-Visible absorption, diffuse reflectance spectroscopy, steady state and time resolved fluorescence spectroscopy. Moreover, the analysed mechanisms and signal changes present similar features both in aqueous solution and on solid nylon support.

This, together with the large dynamic range of the measurement capability, provides high versatility in the potential applications of the presented system. Measurements carried out in water solution gave us the possibility to quantify Cre in micromolar concentrations, while experiments performed on nylon measured the Cre in the millimolar range. For both ranges, typically found in sweat and urine respectively, we analysed the sensor response toward Cre concentrations higher than physiological ones, commonly found in patients with renal diseases.

2. Materials and Methods

2.1 Chemicals and Reagents

Fluorescein sodium (46960), Gold (III) chloride trihydrate ($HAuCl_4 \cdot 3\ H_2O$) (≥ 99.9%, 520918), Sodium tetrachloroaurate dehydrate ($NaAuCl_4 \cdot 2\ H_2O$) (99%, 298174), Creatinine (98%, C4255), Urea (U5378), Valine (≥ 98%, V0500), Leucine (≥ 98%, L8000) were purchased from Sigma- Aldrich. Hydrochloric acid standard solution (343102) was purchased from Fluka. Nylon Amersham Hybond-N + Ge was purchased from Lifesciences.

2.2 Sample preparation for measurements in solution

Fluorescein was dissolved in millipore water to a final concentration of 5 µM. Dye concentration was determined by absorption measurement using a UV–Vis spectrophotometer (Jasco V-760), and an extinction coefficient ε_{473nm}= 92000 $M^{-1} \cdot cm^{-1}$. 50 µL Au^{3+} ions were added to 2.5 mL of the fluorescein solution, previously acidified with HCl at pH 5. The final Au^{3+} ions concentration was 50 µM. Creatinine (43 mM) in aqueous solution was added to the fluorescein-Au^{3+} complex solution at final concentration between 43 µM and 860 µM. 50 µL urea, valine and/or leucine were also added at 860 µM concentration. pH values have always been carefully measured by means of pH indicator strips as VWR 35311.604 (pH 4.5 - 10) and confirmed by measurements by means of a pH meter (Crison) with micro-electrode (HACH, 5208).

2.3 Sample preparation for measurements on solid support

500 µL of fluorescein 0.1 mM and 500 µL of gold 1 mM or 10 mM were mixed in millipore water at two final ratios of 1:10 and 1:100 fluorescein:gold, respectively. 50 µL of the solution were drop casted on nylon support to form yellow spots and they were dried on a thermal plate at 50 °C for 10 minutes. After drying, 30 µL of Creatinine 20 mM, 60 mM, 80 mM were added on the top of the spots and left to dry for 10 minutes.

2.4 Absorption spectra

Absorption spectra were acquired at room temperature in the range 330 – 530 nm using a Jasco V-760 spectrophotometer, in 1 cm path length quartz cuvettes.

2.5 Fluorescence spectra

Fluorescence measurements were acquired at room temperature using a Jasco-FP-8500 spectrofluorometer equipped with a Jasco ETC-815 Peltier as temperature controller in 1 cm path length quartz cuvettes. An excitation bandwidth of 2.5 nm, an emission bandwidth of 2.5 nm, a response time of 1 s, data interval of 0.5 nm, and a scan speed of 100 nm/min were used. Fluorescence emission spectra were acquired, in the range 473 – 650 nm, using λ_{exc}= 473 nm. Fluorescence excitation spectra were acquired, in the ranges 330 – 515 nm and 330 – 530 nm using λ_{em}= 515 nm and λ_{em}= 560 nm, respectively.

2.6 Reflectance spectroscopy

Reflectance spectra on solid nylon-based support were acquired at room temperature using a JASCO V-770 Spectrophotometer equipped with a 60 mm integrating sphere (ISN-923). A sample prepared as in section 2.3 was placed in the solid-state sample holder and measurements were performed in the range 380 – 630 nm by setting a scan speed of 100 nm/min and a bandwidth of 2 nm.

2.7 Fluorescence Lifetime Imaging Microscopy (FLIM)

256×256 pixels FLIM measurements of fluorescein and fluorescein-Au^{3+} complex in solution, before and after Creatinine addition, were collected in the time domain by means of a Leica TCS SP5 inverted microscope coupled with a PicoHarp 300 TCSPC Module (PicoQuant, Berlin, Germany) using a 63×/1.4 oil objective (Leica Microsystems). In this context FLIM measurements are not specifically aimed at imaging but only at measuring the spectroscopic signal of the sample in solution.

Aliquots of aqueous samples were deposited in Chambered Coverglass (Nunc Lab-Tek II) and fluorescein signal wase acquired in the range 505 – 560 nm using excitation at 473 nm from a pulsed White Light Laser (Leica Microsystem) and using λ_{exc} = 780 nm and λ_{exc} = 860 nm for two-photon excitation both lasers have 80 MHz repetition rate.

2.8 FLIM phasor plot analysis and interpretation

The phasor analysis, described by Digman et al.[25], was used for FLIM data. Phasor approach is a technique that allows the translation of the fluorescence decay signal in every pixel of the image to a single point called “phasor” on a polar plot by Fourier transform. In this representation, all possible

single exponential decays lie on the "universal circle" defined as a semicircle, with radius 1⁄2, going from point (0, 0), corresponding to $\tau = \infty$, to point (1, 0), corresponding to $\tau = 0$, where τ is the fluorescence lifetime. Complex decays are represented by phasors within the universal circle. In the phasor plot, it is possible to select the lifetime distributions using coloured cursors. In the original image, the pixels corresponding to a phasor, selected by a coloured cursor, will result with the same colour of the cursor. The images in false colour thus obtained are called "phasor maps". FLIM data have been processed by the SimFCS3 software (Laboratory for Fluorescence Dynamics, University of California, Irvine, CA, available at www.lfd.uci.edu) and FLIM calibration of the system was performed by measuring the known lifetime of the fluorescein in aqueous solution at pH 8 that is a single exponential of 4.0 ns[26].

3. Results

3.1 Fluorescein-Au^{3+} complex formation and Creatinine detection in solution

In the following we report results assessing a proof of concept focused on determining the possibility of using a simple chemical reaction between fluorescein molecules and gold ions for Cre determination using fluorescein signals variations in the optical range.

Figure 1 (a) shows the absorption spectra of fluorescein (5 µM) in water solution at pH 5 before and after Au^{3+} ions addition (50 µM of $HAuCl_4 \cdot 3\ H_2O$ salt) in the range 330 - 530 nm. Fluorescein and gold ions concentrations were selected to optimise the dynamic range in response of Cre additions, and to get absorption values suitable for fluorescence measurements on the very same sample. Analogous measurements in different conditions changing the gold:fluorescein ratios were tested (see Supporting Information figure S1).

In figure 1 (b) fluorescence emission spectra of the same samples, obtained in the range 473 - 650 nm under λ_{exc}= 473 nm, are reported. In line with previous results reported in the literature for aqueous solution at this pH value[27], the absorption spectrum of fluorescein in figure 1 (a) exhibits three characteristic peaks centred at around 390 nm, 447 nm and 473 nm. These peaks result from the presence of fluorescein molecules in different tautomeric forms, which exhibit absorption contributions at different wavelengths [27]. In particular, in these experimental conditions, fluorescein mainly exists in the monoanionic form, but neutral and dianionic species are also present[27,28]. The spectrum of the dianionic form is centred at 490 nm, monoanionic form is characterised by the main

peak at 473 nm together with the small shoulder at 390 nm, while the zwitterionic form is revealed by the presence of a peak centred at 445 nm[27,29]. After Au^{3+} ions addition, the colour of the solution readily undergoes a clear change from bright to pale yellow and this change is immediately evident by visual inspection (see Supporting Information figure S2). The colour change is reflected in large variations in the absorption spectrum. A drastic decrease in the intensity of the whole spectrum is observed and the spectral profile is significantly modified. Specifically, the first absorption peak centred at 390 nm almost disappears, the intensity of the peak at 445 nm is reduced and its position is blue shifted. Furthermore, the intensity of the peak centred at 470 nm decreases and, importantly, a change in the ratio between the intensities (I_{447}/I_{473}) of the last two peaks is also observed. In particular, the measured ratio grows from $I_{447}/I_{473} = 1.01 \pm 0.04$ to $I_{447}/I_{473} = 1.38 \pm 0.06$ suggesting that the monoanionic form is predominantly converted in the zwitterionic one[27]. However, it is not possible to exclude that the dianionic form is also converted into monoanionic and/or zwitterionic ones.

The fluorescence spectrum of fluorescein solution at pH 5 in figure 1 (b) (black line), in line with the literature[27], reveals a broad peak which is representative of the contributions of both dianionic and monoanionic forms since fluorescein in the neutral form does not present a fluorescence signal[30]. Specifically, the emission band at 515 nm is mostly populated by the dianionic form and partially by the monoanionic, while the band at 560 nm by the monoanionic one[30]. From data reported in figure 1 (b), the addition of gold ions (red line) induces a critical reduction in the fluorescence intensity. The fluorescein quantum yield is known to decrease in consequence to the formation of conjugates with other molecules/ions[28]. The observed fluorescence quenching, in accordance with the absorption spectrum changes, suggests that fluorescein forms complex with Au^{3+}. It is possible to speculate that the binding between this dye and gold may involve electron pairs of the oxygen atom present in fluorescein structure[31]. The remaining fluorescence, which comes from free fluorescein molecules, allows the detection of a minimum signal even when all the gold ions are bound. Furthermore, this ensures us that the added Cre reacts with the gold ions complexed with fluorescein molecules. Control measurements using sodium tetrachloroaurate (NaAuCl) were performed to rule out that observed modifications in the absorption/fluorescence spectra of fluorescein are induced by pH (see Supporting Information figure S3). The spectral changes could be ascribed to a base-acid interaction between the deprotonated hydroxyl group of fluorescein molecules and gold ions. Similar mechanisms have been observed for sensors based on quinoline-

modified metal organic framework[31], on Glutathione-capped copper nanoclusters (CuNCs)[32], on Fluorescein- AuNP[23,24]. In these studies, the fluorophore is found to act as an electron donor.

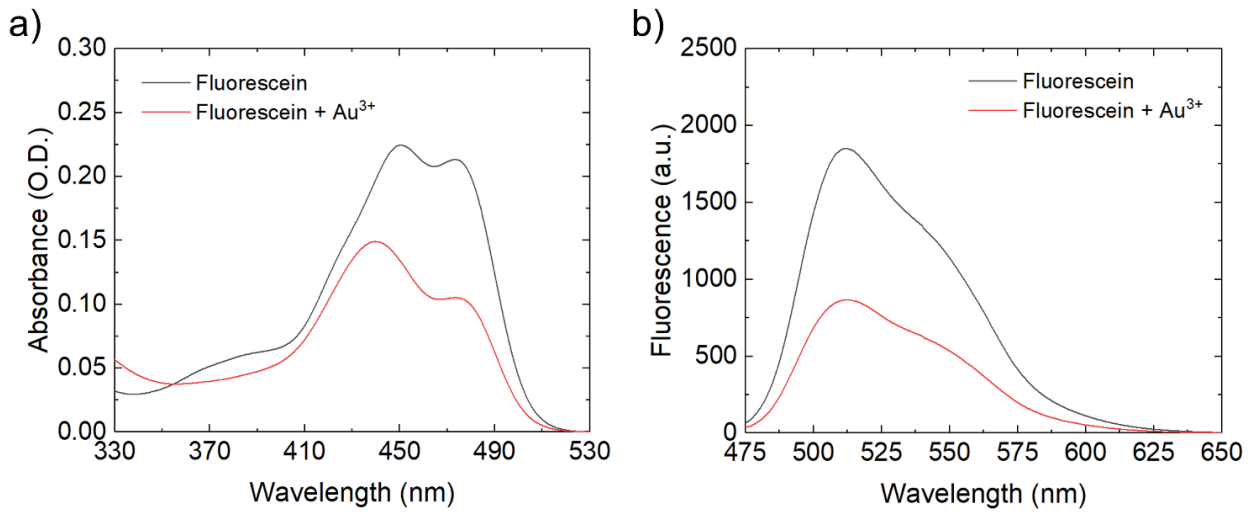

Fig 1. (a) Absorption spectra, acquired in the range 330 nm – 530 nm, of fluorescein 5 µM concentration dissolved in water solution pH 5 before (black line) and after (red line) the addition of 50 µM of gold ions. (b) Fluorescence emission spectra of fluorescein (5 µM) dissolved in water solution pH 5 before (black line) and after (red line) the addition of 50 µM of gold ions (λ_{exc}= 473 nm, acquisition range 473 nm – 650 nm). Spectral changes are attributed to fluorescein-Au^{3+} complex formation. These experiments were repeated more than five times.

Figure 2 (a) shows absorption spectra of fluorescein dye-Au^{3+} ion conjugate before (red line – spectrum at lower intensity) and after the addition of Cre at increasing concentration ranging from 43 µM to 860 µM. In figure 2 (b) the corresponding fluorescence spectra are reported, while panel 2 (c) shows the fluorescence intensity at 515 nm as a function of Cre concentration. To highlight spectral shape modifications, we also reported in figure 2 (d) the measured fluorescence spectra normalized to their maximum value. It is worth noting that spectral changes occur almost instantaneously and, after that, the signal remains stable.

As shown in panel 2 (a), at increasing Cre concentration, the intensity of the peaks at 390 nm, 447 nm, and 473 nm grows and the I_{447}/I_{473} ratio is inverted going from I_{447}/I_{473} = 1.38 ± 0.06 to I_{447}/I_{473} = 0.91 ± 0.04. Progressive spectral changes toward free fluorescein typical shape (figure 1 (a)) are observed. These modifications suggested that the coordination bond between fluorescein and Au^{3+} is progressively destabilised in presence of Cre and that free fluorescein molecules, released by the dissociation of the complex, modify the absorption spectrum. It may indicate that the Lewis base Cre has a stronger affinity toward the Lewis acid Au^{3+}, so that Cre competes with the dye in bonding Au^{3+}. Cre is characterized by a higher pK_a value than fluorescein, making the Cre more available to

give up its free electrons to form bonds. It is important to note that in the presented conditions, the pH value, even at the highest Cre concentration (860 μM), does not notably change. Figure S4 (see Supporting Information) reports the plot of the absorption intensity of the peak at 475 nm as a function of Cre concentration in the range 43 μM – 350 μM. These data reveal a linear response of the sensor toward Cre concentration. It is possible to detect this analyte concentration through absorption measurements, but results, obtained by fluorescence measurements and reported in figure 2 (b) and figure 2 (c), show higher sensitivity. As it is clear in figure 2 (b), Cre presence triggers the turn-on of fluorescence: the intensity gradually grows as the concentration of the analyte increases, reaching intensity values comparable to the one of free fluorescein in solution.

The formation of Lewis acid-base complexes between Cre and Au^{3+} would lead to the interruption of energy transfer and electron transfer from fluorescein to Au^{3+} and the consequential recovery of fluorescein quenching caused by Au^{3+} [31]. This mechanism of action was also proposed in previous works to explain Cre detection[31]. Figure 2 (c) shows the value of fluorescence intensity maxima as a function of Cre concentrations. A biphasic behaviour is observed. The growth of fluorescence intensity measured at 515 nm can be approximated in two different linear regions. The first between 43 μM and 344 μM, with a slope of 3.3 ± 0.1 while at higher Cre concentrations, the fluorescence enhancement is reduced (slope = 0.94 ± 0.05).

In figure 2 (d), the normalized fluorescence spectra to their maximum intensity are reported. These data highlight that the growth of fluorescence intensity occurring at increasing Cre concentration is coupled with a reduction of the spectral width. This is mainly due to the fact that, as reported above, the fluorescein monoanionic and dianionic forms contribute to the fluorescence spectrum[27] and that the ratio between the monoanionic form (which falls at higher wavelengths) and the dianionic form decreases increasing Cre concentration. The dependence of the total fluorescence intensity on Cre concentration is reported in figure S5 and presents a similar biphasic behaviour, where the dependence of fluorescence intensity on Cre concentration for values above 400 μM is smaller than the one observed in panel 3 (c) and reaches a plateau above 600 μM.

Importantly for applied purposes a better efficiency of sensing is achieved when measuring fluorescence intensity variations at single wavelength close to the peak maximum (λ=515 nm). This enabled us to identify two different linear regions where Cre can be detected with high sensitivity roughly selecting in somehow the contribution to the emission of dianionic species. From a practical point of view, the use of a single wavelength detector may represent a faster, simpler and more selective technological solution.

Small spectral changes observed in the red part of the fluorescence spectrum may lead to the hypothesis that the monoanionic form of fluorescein progressively decreases due to the release of gold and/or the deprotonation of hydroxylic groups of fluorescein. We also reported, in the supplementary material figure S6, the fluorescence excitation spectra. These data are useful to investigate which absorption transitions populate the excited states responsible for the fluorescence bands at about lower (515 nm) and higher wavelength (560 nm) and further confirm the formation of fluorescein-Au^{3+}complex. Furthermore, they support the hypothesis that the Cre induces the dissociation of the complex and the release of fluorescein in the dianionic form.

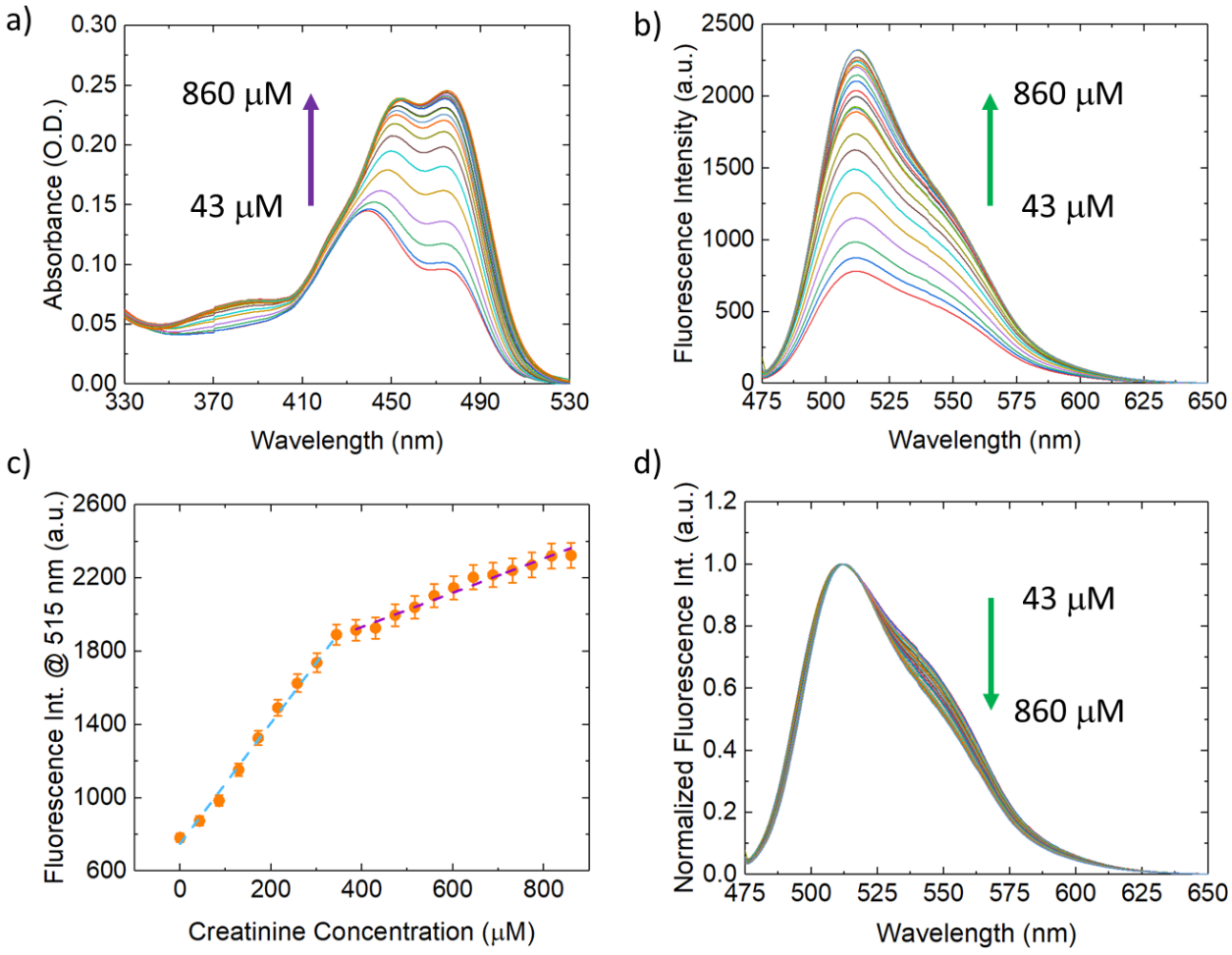

Fig 2. (a) Absorption spectra (range 330 nm – 530 nm) of fluorescein-Au^{3+} complex before (red line) and after the addition of Cre in concentrations ranging from 43 µM to 860 µM. (b) Fluorescence emission spectra of fluorescein-Au^{3+} complex before (red line) and after the addition of increasing Cre concentrations (range = 43 µM - 860 µM), acquired between 473 nm and 650 nm (λ_{exc}= 473 nm). (c) Fluorescence intensity measured at 515 nm as a function of increasing Cre concentrations, dashed lines indicate different ranges of linearity that can be used for creatinine detection. (d) Fluorescence spectra normalized to their maximum value in order to highlight the band reduction of fluorescence contribution at higher wavelengths with increasing Cre concentrations. All the experiments were repeated more than five times.

In figure 3 the phasor analysis of FLIM measurements on fluorescein and fluorescein-Au^{3+} complex, before and after the addition of Cre 860 μM, are reported. Fluorescence lifetime depends exclusively on the environment surrounding the fluorophore, being insensitive to variations in excitation source intensity, detector gain setting and importantly on sample fluorophore concentration. Therefore, it is a powerful tool to avoid experimental artefacts that can arise by analysing only the fluorescence intensity. The signal was sequentially acquired in the range 505 - 560 nm, under excitation at three different wavelengths (λ_{exc} = 473 nm, λ_{exc} = 780 nm and λ_{exc} = 860 nm). Two-photon excitations at λ_{exc} = 780 nm and λ_{exc} = 860 nm are used to investigate UV spectral regions with minimal perturbation of the sample. FLIM measurements on solution samples are only meant at giving a graphical representation of the data. As expected, no structures over the diffraction limited resolution are found and only uniformly diffused fluorescence is observed so that images appear as uniformly coloured. Aim of these measurements is to separate the contribution of different excitation levels and to highlight relevant interactions in the observed sensing capability. For each excitation wavelength, three representative 256×256 pixels images (phasor maps) and a phasor plot are reported.

Figure 3 (a) shows the phasor maps and the phasor plot of fluorescein, fluorescein-Au^{3+}, and the complex after Cre addition, under two-photon excitation at 780 nm, which would correspond to the absorption peak at 390 nm. At this wavelength, fluorescein monoanionic form is preferentially excited but the dianionic form is also excited in minor fraction[29]. The expansion of the phasor region is shown in the dotted box. For each measurement, pixels with specific lifetime were selected in the phasor plot using a coloured circle and corresponding pixels appear coloured with the same colour code on the phasor maps. In phasor plot two lifetime distributions are distinguishable on the universal circle, characterised by an average lifetime of about τ=3.9 ns and τ= 3.3 ns, highlighted by red and green circles, respectively. Similar lifetime values are reported in literature for fluorescein in the dianionic (τ= 4.1 ns) and the monoanionic forms (τ= 3 ns)[30]. Data in figure 3 (a) show that free fluorescein at pH 5 is characterised by a fluorescence lifetime distribution centred at about 3.9 ns; this reflects in a correspondent phasor map uniformly coloured in red. After the addition of gold ions, the lifetime distribution of the fluorescein-Au^{3+} complex shifts to shorter lifetime (about 3.3 ns) resulting in a phasor map uniformly coloured in green. The presence of Cre in solution brings back the measured lifetime distribution to the initial value characteristic of free fluorescein. Again, data indicate that gold ions interact with the deprotonated hydroxyl groups present in the

fluorescein dianonic and monoanionic form, and induce the decrease of fluorescein lifetime to a value of 3.3 ns. This value predominantly corresponds to the lifetime of fluorescein molecule in its monoanionic form. The presence of Cre restores the initial conditions, bringing the phasor back to a position corresponding to a value of 3.9 ns. Panels 3 (b) and (c) show the phasor maps and phasor plots when the sample is excited at λ_{exc} = 860 nm (corresponding to two-photon excitation of the transition at about λ_{exc} = 447 nm) and at λ_{exc} = 473 nm, respectively. Under these excitation wavelengths, fluorescence lifetime does not considerably change and consequently the phasor maps do not change colour. The measured lifetime distribution is centred at 3.5 ns. This lifetime value falls in intermediate values between the values of the two distinct forms. These data could suggest that the intensity differences of the peaks at 447 nm and 473 nm, revealed by absorption measurements (figure 1 (a) and figure 2 (a)), could be attributable only to the different number of tautomeric forms in solution. On the contrary, the changes of lifetime, observed under excitation at 780 nm, indicate that the electronic level associated with this transition is directly involved in bonding with gold ions.

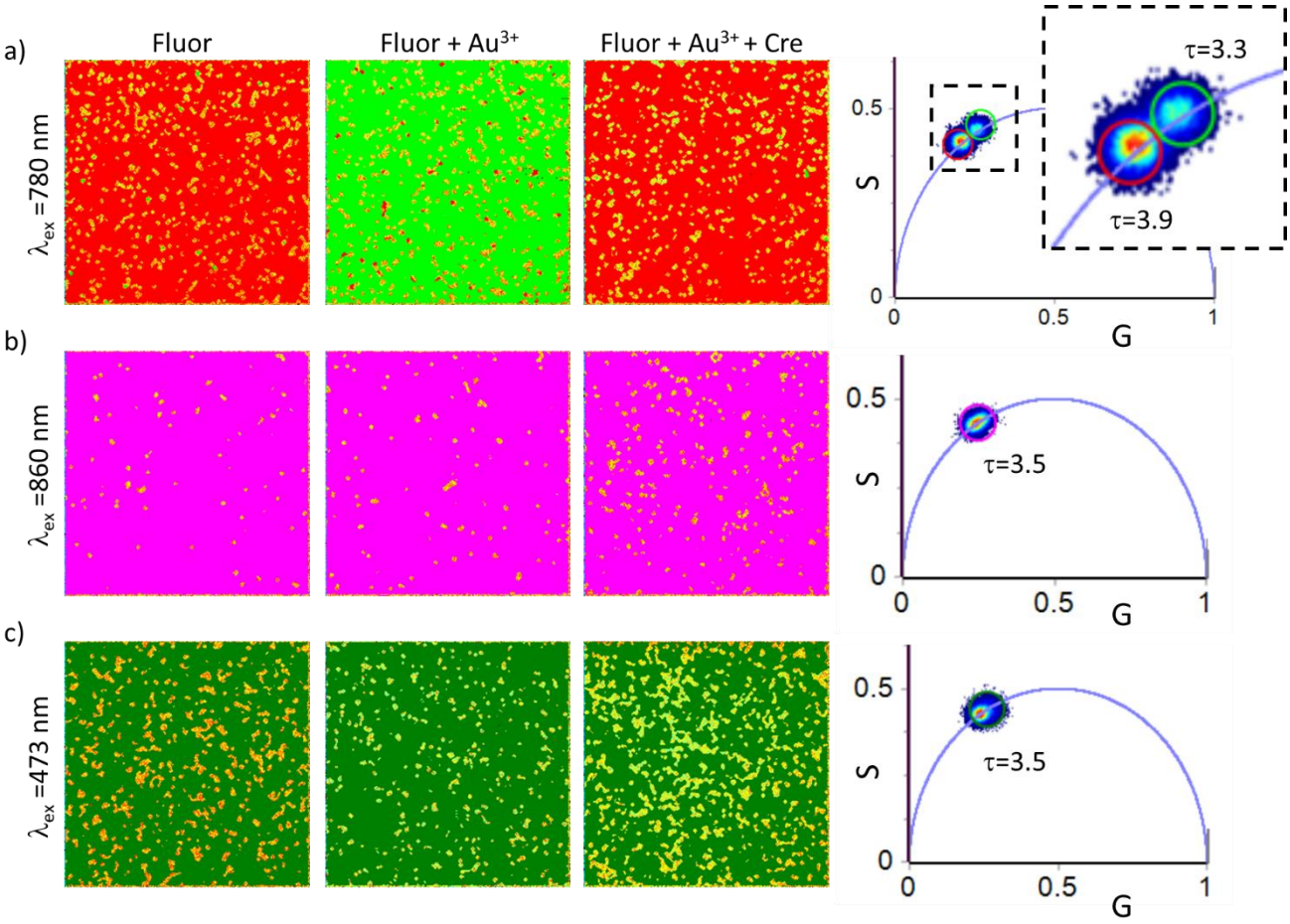

Fig 3. Phasor analysis of 256 × 256 pixels FLIM measurements on Fluorescein (5 µM) and Fluorescein-Au^{3+} (in a ratio 1:10) conjugates before and after the addition of Cre (860 µM). Measurements were collected in the range 505 nm-560 nm under three different excitation wavelengths (λ_{exc}=473 nm, λ_{exc}=780 nm and λ_{exc}=860 nm). The fluorescence lifetime distributions obtained from each measurement and reported in the respectively phasor plots are highlighted by coloured cursors whose size and the position are arbitrary. Each pixel of the phasor colour maps is coloured according to the colour of the corresponding cursor in the phasor plots. The magnification of fluorescein lifetime distributions after the excitation of the samples at 780 nm, is reported in the dashed lines surrounded inset. These experiments were performed in triplicates.

The overall information obtained from the spectral steady state and time resolved fluorescence data denote the formation of a complex between fluorescein and gold ions that could be stabilised via coordination interactions[31]. Cre molecules compete with fluorescein in binding the Au^{3+} ions and specifically Cre in solution destabilises the fluorescein-Au^{3+} complex inducing the release of free fluorescein in the dianionic and monoanionic forms.

This simple and highly repeatable chemical reaction is reflected in evident colour changes of the solution and in critical changes of absorption and fluorescence spectra and lifetime. These changes can be quantified and calibrated, and present a linear trend that can be highlighted in different concentration ranges. The slope of the corresponding lines indicates a different sensitivity for each range (see e.g. cyan and purple dashed lines in figure 2 (c)). A linear response in the measured signal is obtained for Cre concentrations between 43 µM and 344 µM with a higher slope with respect to the one found in the range 400 µM – 860 µM. These measurable concentration ranges may be applied to Cre quantification in sweat and numerous studies have already focused on trying to quantify Cre in this matrix [38,39]. A quick and reliable analysis of this fluid is highly desirable also in view of the realisation of wearable sensors[39,43] which may allow to instantaneous and continuous diagnosis during normal day-to-day activities.

Sweat fluid can contain several biochemical markers of clinical interest, and comprises the natural route for the excretion of biological waste products. For this reason, it is possible to find in sweat, in addition to Cre, other human excreted products like urea, valine, leucine, histidine, lysine, and threonine[40-42]. In this context, it is important to verify the selectivity of fluorescein- Au^{3+} complex for specific recognition of Cre. In order to do that, we report in figure 4 (a) the absorption spectra of fluorescein- Au^{3+} in the presence of 860 µM Cre, 860 µM leucine (Leu), 860 µM valine (Val), 860 µM Urea. These small molecules were selected as suitable models as they are present in the biological fluid of interest. As can be seen only the addition of Cre significantly modify the spectral profile.

In figure 4 (b), the absorption spectrum of fluorescein-Au^{3+}, in the presence of a mix of the same components (860 µM Leu, 860 µM Val and 860 µM Urea), is compared to the spectrum of the same sample after the addition of 860 µM Cre which reveals the expected spectral changes. The comparison of data in figure 4 (a) and (b) confirm that the spectral modifications are the same both in the presence and in the absence of other biomolecules and that only the addition of Cre induces spectral modifications. To further support these results, in figure S7 analogous measurements using other potentially interacting aminoacids are reported.

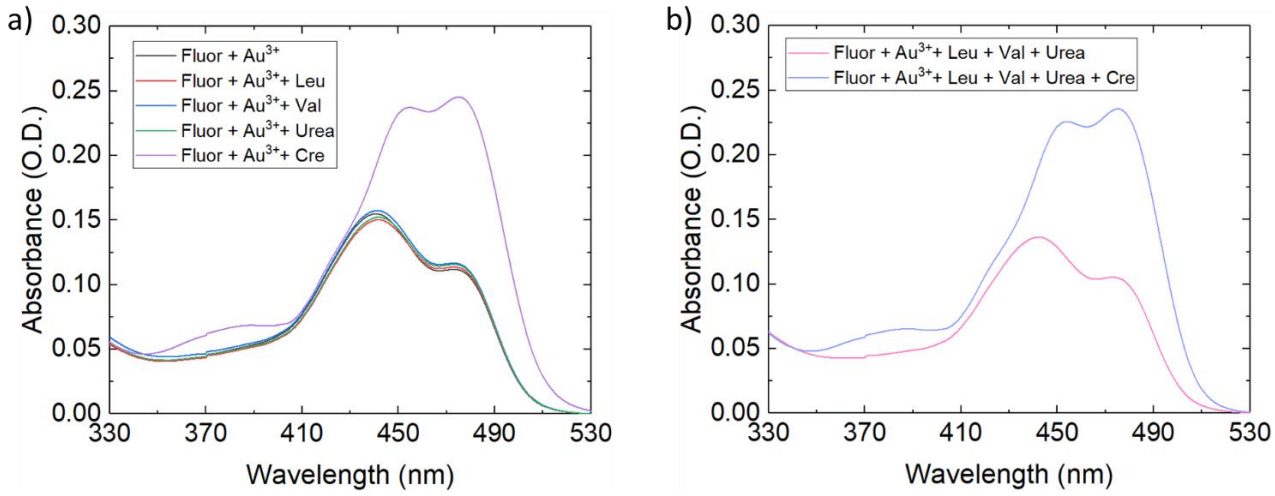

Fig 4. Fluorescein-Au^{3+} complex absorption spectra in the range 330 nm – 530 nm (a) before and after addition of 860 µM Leu (red line), 860 µM Val (blue line), 860 µM Urea (green line) and 860 µM Cre (violet line), and (b) in presence of Leu, Val, Urea mixed together, before (pink line) and after (light blue line) Cre addition. The concentration of each analyte is 860 µM. These data reveal that the fluorescein-Au^{3+} complex is selective for Cre detection.

3.2 Creatinine detection on nylon support

The spectroscopic analysis of the ligand exchange reaction between the fluorescein-Au^{3+} complex with Cre demonstrated its effectiveness for Cre detection in solution in a concentration dependent manner. In particular, Cre addition to fluorescein-Au^{3+} complex solution determines a change in the absorption spectrum. Changes in the visible range (above 400 nm) can be exploited to design a colorimetric point-of-care test for Cre detection in a solid format. To this aim, we designed a colorimetric sensor obtained by the deposition of fluorescein-Au^{3+} complex on a nylon substrate, and the Cre analyte was directly dropped on the complex spot to detect the change in colour due to ligand exchange. The sensor was intended to detect harmful levels of Cre in urine (upper unphysiological range > 20 mM)[2], and the optical variations were followed by UV-Vis diffuse

reflectance spectroscopy. Nylon was selected as suitable substrate for this approach because of its porosity in the microscale that allows the immobilization of a proper amount of fluorescein-Au^{3+} complex respect to a flat support by imbibition[33], whiteness, ideal for reflectance measurements, flexibility and inexpensiveness.

In figure 5 (a) the diffuse reflectance spectra of the fluorescein-Au^{3+} complex on nylon, upon addition of Cre at increasing concentration up to 80 mM, are reported together with the spectrum of the fluorescein-Au^{3+} prior to the addition. As evident, the typical two peaks shape characterizes the reflectance spectrum of the complex, before Cre addition. Diffuse reflectance signal increases and the spectrum slightly shifts to higher wavelengths. The spectral features, highlighted in figure 5 (a), reflect the ones previously shown in figure 2 (a) obtained by measurements performed in solution. Detailed differences in peak position and width can be related to the different state of the molecules immobilized on the nylon support, with respect to the related system in aqueous solution. Interestingly, also in the solid state an analogous behaviour to the one observed in solution is observed. Dropping Cre at increasing concentrations on the fluorescein-Au^{3+} spot causes an immediate, evident and stable colour change, which corresponds to an overall decrease in reflectance intensity, corresponding to higher absorbance in solution spectra.

In addition, similar changes in shape and maxima intensity ratio were observed at increasing Cre concentration, with a decrease of the band at 464 nm, and an increase and shift of the band at 492 nm up to 507 nm after Cre 80 mM addition. These data confirm the possibility to carry out the ligand exchange reaction between the fluorescein-Au^{3+} complex with Cre on nylon and the similarity of the chemical process investigated in aqueous solution.

In order to improve the Cre sensor applicability towards the establishment of a colorimetric screening test, we investigated the possibility to determine a more evident change in colour. To obtain this result, the fluorescein:Au^{3+} molar ratio was modified from 1:10 to 1:100 to coordinate a higher amount of fluorescein molecules in the initial spot.

In figure 5 (b), the higher concentration of Au^{3+} ions determine drastic changes in the reflectance spectrum of the complex spot before the addition of the creatinine, consisting in the presence of a unique band with a minimum at 450 nm. The addition of an increasing amount of Cre determines the expected spectral changes with a decrease of the complex signal intensity at 450 nm along with an increase of the component at 492 nm. Comparing the sensors obtained at fluorescein:Au^{3+} 1:10 and 1:100 molar ratio, the ΔR between the reflectance absolute minima after creatinine reaction is improved from 28 nm to 42 nm, which results in more evident change in colour by eyes. The diffuse

reflectance spectrum of fluorescein (dashed) was also reported as reference, to highlight the release of free fluorescein molecules as a result of the ligand exchange reaction with Cre.

In addition, the reflectance data were computed to show the evidence of the change in colour of the sensor after the reaction with Cre on a tristimulus colour space[34]. This approach is useful to highlight the colour of samples deposited on solid substrates[35,36]. In figure 5 (c) we reported the chromaticity diagram (CIE 1930), showing the colour components change at different Cre concentrations. Before the reaction with Cre, the fluorescein-Au^{3+} complex dot on the chromaticity diagram is on the yellow area. Upon Cre addition, the dot position shifts towards free fluorescein in the orange area with an extent related to the Cre concentration. Figure 5 (d) shows the photographic images of nylon supports loaded with fluorescein-Au^{3+} before and after Cre addition.

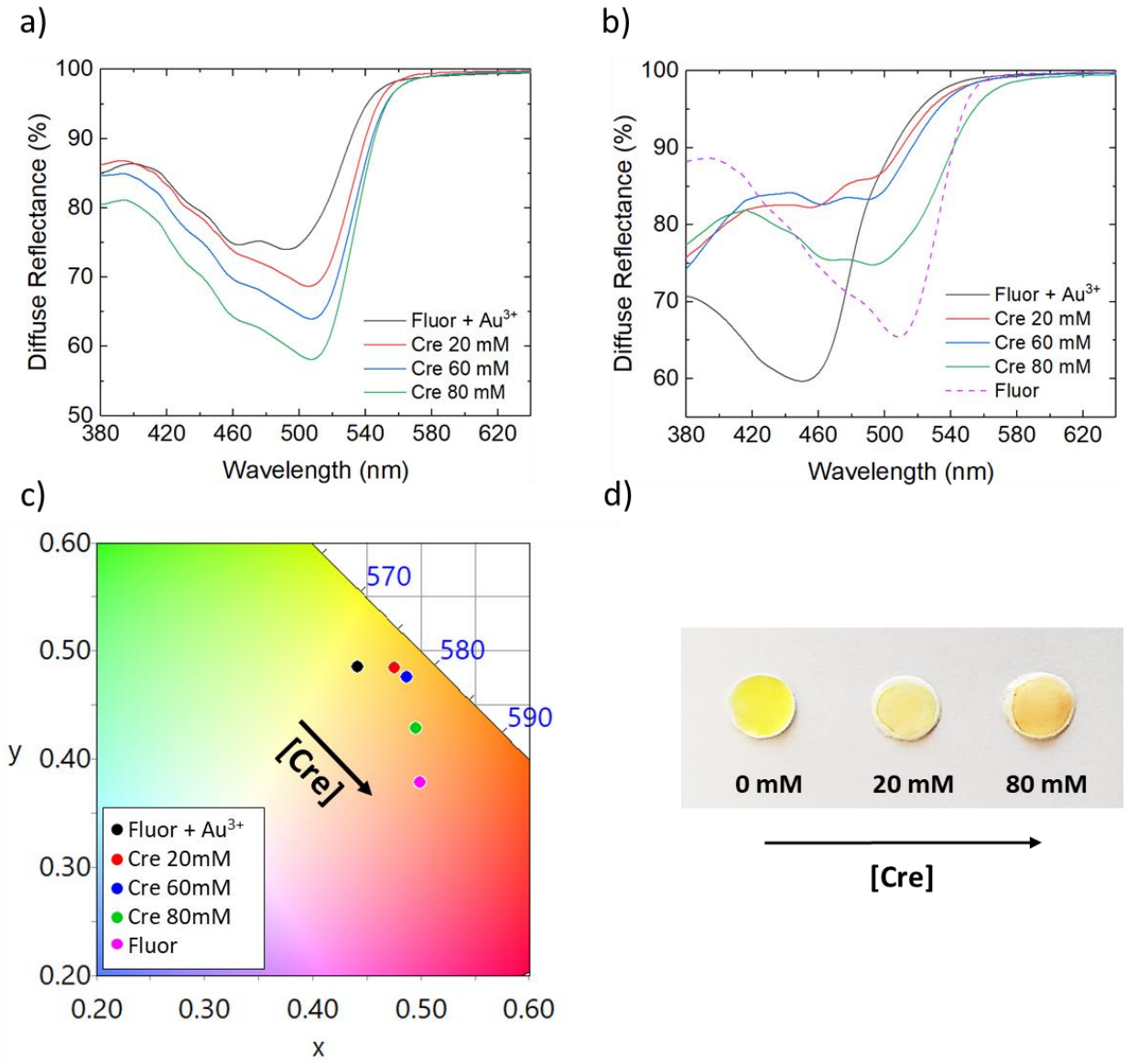

Fig 5. (a-b) Fluorescein-Au^{3+} complexes reflectance spectra, acquired in the range 380 nm – 630 nm, before and after the addition of increasing Cre concentrations; fluorescein:gold ratio is 1:10 and 1:100 in (a) and (b), respectively. (c) Chromaticity diagram (CIE 1930) showing the colour components change at different Cre concentrations. (d) Photographic images of nylon loaded with fluorescein-Au^{3+} complex in absence and in presence of 20 mM and 80 mM concentrations of Cre. A visible colour change from yellow to orange is observed that is proportional to Cre concentrations. These experiments were repeated in triplicates.

The photographs reveal that the fluorescein-Au^{3+} complexes, dropped on the nylon supports, change colour in presence of Cre concentrations above physiological values found in urine. We assist an instantaneous colour change from yellow to orange, visible by naked eyes, that is more evident at higher Cre concentrations.

As a future perspective, the use of the fluorescein-Au^{3+} complex on solid-nylon supports could allow the development of a rapid, not invasive, and preliminary homemade diagnosis of renal suffering.

4. Conclusions

Detecting Cre levels in biological fluids is clinically important because levels of this analyte outside of typical ranges are the evidence of health issues associated with renal and muscular functioning. In this study, we have presented a multiplexed assay for the rapid Cre detection based on competitive association of Cre and fluorescein with Au^{3+} ions. Absorbance and fluorescence data indicate that fluorescein-Au^{3+} complex, in the presence of Cre, dissociates towards the formation of Cre-Au^{3+} complex allowing the releasing of free fluorescein in solution. The presence of free fluorescein results in a drastic increase of fluorescence emission previously partially quenched by the complexation with Au^{3+} ions. Changes of the ratio between the populations (neutral, monoanionic and dianionic) of fluorescein, generated by the bonding/unbonding of Au^{3+} ions, can be monitored by means of UV-Visible absorption, diffuse reflectance spectroscopy and steady state and time resolved fluorescence spectroscopy.

The formation of a complex between fluorescein and gold ions, possibly stabilised via coordination interactions[31], is at the basis of the observed Cre sensing. Indeed, data reveal that Cre molecules compete with fluorescein binding to Au^{3+} ions, destabilising the fluorescein-Au^{3+} complex, inducing the release of free fluorescein and thus modifying the ratio between dianionic and anionic species in the sample. This results in large modification in the observed optical properties so that Cre can be easily quantified both using absorption and fluorescence spectroscopy, giving reliable results also through measurements at single wavelength.

Measurements in aqueous solution at pH 5 revealed a linear response of fluorescein-Au^{3+} complex towards micromolar concentrations of Cre that are the typical conditions of pH and concentration found in sweat. As a future perspective and by exploiting microfluidics technology[37], these results may be translated into comfortable and cost-effective commercial wearable sensors which have the ability to directly monitor Cre from biofluids in a non-invasive manner. The analysed sensing solution, in semipermeable compartments or channels, may be at the basis of the building block of flexible transparent patches to monitor Cre levels in sweat. The different read outs may pave the way to design different specific integrated devices with tunable dynamic range and sensitivity.

Interestingly, the same system revealed suitable sensing capability in the dry state allowing the development of a colorimetric sensor with sensitivity in the millimolar range values that are found in urine fluids. This is obtained by drop casting the fluorescein-Au^{3+} complex on solid and flexible

nylon support. A visible colour change from yellow to orange of the nylon sensor is observed in presence of pathological Cre concentrations (> 20 mM), i.e. as the Cre level deserves clinical attention. A proof of concept is given based on these results which may constitute the base for a selective colorimetric screening test, easily usable at home, for a rapid and preliminary diagnosis of renal dysfunction by monitoring Cre in urine.

5. Acknowledgments

Financial support from the PNR 2015-2020 - 4Frailty – ARS01_00345 and from PON AIM1809078-1 is acknowledged.

Conflict of interest

The authors declare no conflict of interest.

Author contributions

Sara Anselmo: Conceptualization, Formal analysis, Investigation, Methodology, Visualization, Writing. Giuseppe De Luca: Formal analysis, Investigation, Methodology, Visualization, Writing-. Vittorio Ferrara: Formal analysis, Investigation, Methodology, Visualization, Writing. Bruno Giuseppe Pignataro: Funding acquisition, Methodology, Resources, - review & editing.

Giuseppe Sancataldo: Conceptualization, Funding acquisition, Methodology, Project administration, Resources, Writing - review & editing. Valeria Vetri: Conceptualization, Funding acquisition, Methodology, Project administration, Resources, Writing - review & editing.

References

1. Balestrino M. Role of Creatine in the Heart: Health and Disease. *Nutr 2021, Vol 13, Page 1215*. 2021;13(4):1215. doi:10.3390/NU13041215
2. Cánovas R, Cuartero M, Crespo GA. Modern creatinine (Bio)sensing: Challenges of point-of-care platforms. *Biosens Bioelectron*. 2019;130:110-124. doi:10.1016/J.BIOS.2019.01.048
3. Walsh DA, Dempsey E. Comparison of electrochemical, electrophoretic and spectrophotometric methods for creatinine determination in biological fluids. *Anal Chim Acta*. 2002;459(2):187-198. doi:10.1016/S0003-2670(02)00110-1
4. Li M, Du Y, Zhao F, Zeng J, Mohan C, Shih W-C. Reagent- and separation-free measurements of urine creatinine concentration using stamping surface enhanced Raman scattering (S-SERS). *Biomed Opt Express*. 2015;6(3):849. doi:10.1364/BOE.6.000849
5. Harlan R, Clarke W, Di Bussolo JM, Kozak M, Straseski J, Meany DL. An automated turbulent flow liquid chromatography–isotope dilution mass spectrometry (LC–IDMS) method for quantitation of serum creatinine. *Clin Chim Acta*. 2010;411(21-22):1728-1734. doi:10.1016/J.CCA.2010.07.013
6. Lee HL, Chen SC. Microchip capillary electrophoresis with electrochemical detector for precolumn enzymatic analysis of glucose, creatinine, uric acid and ascorbic acid in urine and serum. *Talanta*. 2004;64(3):750-757. doi:10.1016/J.TALANTA.2004.03.046
7. Dal Dosso F, Decrop D, Pérez-Ruiz E, et al. Creasensor: SIMPLE technology for creatinine detection in plasma. *Anal Chim Acta*. 2018;1000:191-198. doi:10.1016/J.ACA.2017.11.026
8. Guinovart T, Hernández-Alonso D, Adriaenssens L, et al. Recognition and Sensing of Creatinine. *Angew Chem Int Ed Engl*. 2016;55(7):2435-2440. doi:10.1002/ANIE.201510136
9. Duong HD, Rhee J Il. Development of Ratiometric Fluorescent Biosensors for the Determination of Creatine and Creatinine in Urine. *Sensors 2017, Vol 17, Page 2570*. 2017;17(11):2570. doi:10.3390/S17112570
10. Pal S, Lohar S, Mukherjee M, Chattopadhyay P, Dhara K. A fluorescent probe for the selective detection of creatinine in aqueous buffer applicable to human blood serum. *Chem Commun*. 2016;52(94):13706-13709. doi:10.1039/C6CC07291G
11. Ellairaja S, Shenbagavalli K, Vasantha VS. Ultrasensitive Fluorescent Biosensor for Creatinine Determination in Human Biofluids Based on Water Soluble Rhodamine B Dye-Au3+ ions Conjugate. *ChemistrySelect*. 2017;2(3):1025-1031. doi:10.1002/SLCT.201601110
12. Alula MT, Karamchand L, Hendricks NR, Blackburn JM. Citrate-capped silver nanoparticles as a probe for sensitive and selective colorimetric and spectrophotometric sensing of creatinine in human urine. *Anal Chim Acta*. 2018;1007:40-49. doi:10.1016/J.ACA.2017.12.016
13. Abedalwafa MA, Li Y, Ni C, Wang L. Colorimetric sensor arrays for the detection and identification of antibiotics. *Anal Methods*. 2019;11(22):2836-2854. doi:10.1039/C9AY00371A
14. Erenas MM, Ortiz-Gómez I, De Orbe-Payá I, et al. Ionophore-based optical sensor for urine creatinine determination. *ACS Sensors*. 2019;4(2):421-426. doi:10.1021/ACSSENSORS.8B01378/SUPPL_FILE/SE8B01378_SI_001.PDF
15. Andrés A, Sierra F, Hernándezhernández-Alonso D, et al. Optical Supramolecular Sensing of Creatinine. *J Am Chem Soc*. 2020;142:4284. doi:10.1021/jacs.9b12071
16. Sittiwong J, Unob F. Detection of urinary creatinine using gold nanoparticles after solid phase extraction. *Spectrochim Acta Part A Mol Biomol Spectrosc*. 2015;138:381-386.

doi:10.1016/J.SAA.2014.11.080
17. He Y, Zhang X, Yu H. Gold nanoparticles-based colorimetric and visual creatinine assay. *Microchim Acta*. 2015;182(11-12):2037-2043. doi:10.1007/S00604-015-1546-0/FIGURES/7
18. Piriya V.S A, Joseph P, Daniel S.C.G. K, Lakshmanan S, Kinoshita T, Muthusamy S. Colorimetric sensors for rapid detection of various analytes. *Mater Sci Eng C*. 2017;78:1231-1245. doi:10.1016/J.MSEC.2017.05.018
19. Lee NY, Jung YK, Park HG. On-chip colorimetric biosensor based on polydiacetylene (PDA) embedded in photopolymerized poly(ethylene glycol) diacrylate (PEG-DA) hydrogel. *Biochem Eng J*. 2006;29(1-2):103-108. doi:10.1016/J.BEJ.2005.02.025
20. Abou-Zied OK, Sulaiman SAJ. Site-specific recognition of fluorescein by human serum albumin: A steady-state and time-resolved spectroscopic study. *Dye Pigment*. 2014;110:89-96. doi:10.1016/J.DYEPIG.2014.05.005
21. Chen SC, Nakamura H, Tamura Z. Studies on the Metabolites of Fluorescein in Rabbit and Human Urine. *Chem Pharm Bull*. 1980;28(5):1403-1407. doi:10.1248/CPB.28.1403
22. Slavík J. Applications of fluorescent probes in cellular biology measurement of intracellular pH. *J Lumin*. 1997;72-74:575-577. doi:10.1016/S0022-2313(96)00401-2
23. Nebu J, Anjali Devi JS, Aparna RS, Aswathy B, Lekha GM, Sony G. Fluorescence turn-on detection of fenitrothion using gold nanoparticle quenched fluorescein and its separation using superparamagnetic iron oxide nanoparticle. *Sensors Actuators B Chem*. 2018;277:271-280. doi:10.1016/J.SNB.2018.08.153
24. Hormozi-Nezhad MR, Bagheri H, Bohloul A, Taheri N, Robatjazi H. Highly sensitive turn-on fluorescent detection of captopril based on energy transfer between fluorescein isothiocyanate and gold nanoparticles. *J Lumin*. 2013;134:874-879. doi:10.1016/J.JLUMIN.2012.06.032
25. Digman MA, Caiolfa VR, Zamai M, Gratton E. The Phasor Approach to Fluorescence Lifetime Imaging Analysis. *Biophys J*. 2008;94(2):L14-L16. doi:10.1529/BIOPHYSJ.107.120154
26. Data Tables | Fluorescence Lifetime Standards | ISS. http://www.iss.com/resources/reference/data_tables/FL_LifetimeStandards.html. Accessed June 16, 2021.
27. Gerasimova MA, Tomilin FN, Malyar EY, et al. Fluorescence and photoinduced proton transfer in the protolytic forms of fluorescein: Experimental and computational study. *Dye Pigment*. 2020;173:107851. doi:10.1016/J.DYEPIG.2019.107851
28. Wang L, Roitberg A, Meuse C, Gaigalas AK. Raman and FTIR spectroscopies of fluorescein in solutions. *Spectrochim Acta Part A Mol Biomol Spectrosc*. 2001;57(9):1781-1791. doi:10.1016/S1386-1425(01)00408-5
29. Alvarez-Pez JM., Ballesterons L, Talavera E, Yguerabide J. Fluorescein Excited-State Proton Exchange Reactions: Nanosecond Emission Kinetics and Correlation with Steady-State Fluorescence Intensity. *The Journal of Physical Chemistry A.* 2001;105(26):6320-6332. doi: 10.1021/jp010372+
30. Sjöback R, Nygren J, Kubista M. Absorption and fluorescence properties of fluorescein. *Spectrochim Acta Part A Mol Biomol Spectrosc*. 1995;51(6):L7-L21. doi:10.1016/0584-8539(95)01421-P
31. Qu S, Cao Q, Ma J, Jia Q. A turn-on fluorescence sensor for creatinine based on the quinoline-modified metal organic frameworks. *Talanta*. 2020;219. doi:10.1016/J.TALANTA.2020.121280
32. Jalili R, Khataee A. Aluminum(III) triggered aggregation-induced emission of glutathione-capped copper nanoclusters as a fluorescent probe for creatinine. *Microchim Acta*.

2019;186(1):1-9. doi:10.1007/S00604-018-3111-0/TABLES/3
33. Arrabito G, Ferrara V, Ottaviani A, et al. Imbibition of Femtoliter-Scale DNA-Rich Aqueous Droplets into Porous Nylon Substrates by Molecular Printing. *Langmuir*. 2019;35(52):17156-17165. doi:10.1021/ACS.LANGMUIR.9B02893/SUPPL_FILE/LA9B02893_SI_002.AVI
34. Pridmore RW. Complementary colors: A literature review. *Color Res Appl*. 2021;46(2):482-488. doi:10.1002/COL.22576
35. Singh V, Mishra AK. White Light Emission from Vegetable Extracts. *Sci Reports 2015 51*. 2015;5(1):1-9. doi:10.1038/srep11118
36. Aleeva Y, Ferrara V, Bonasera A, Martino DC, Pignataro B. Superhydrophobic TiO2/fluorinated polysiloxane hybrid coatings with controlled morphology for solar photocatalysis. *Colloids Surfaces A Physicochem Eng Asp*. 2021;631. doi:10.1016/J.COLSURFA.2021.127633
37. Vinoth R, Nakagawa T, Mathiyarasu J, Mohan AMV. Fully Printed Wearable Microfluidic Devices for High-Throughput Sweat Sampling and Multiplexed Electrochemical Analysis. *ACS Sensors*. 2021;6(3):1174-1186. doi:10.1021/ACSSENSORS.0C02446/SUPPL_FILE/SE0C02446_SI_005.AVI
38. Zhang Y, Guo H , Kim S., Wu Y, Ostojich D, Park S H, Wang X , Weng Z, Li R , Bandodkar A. J, Sekine Y, Choi J, Xu S, Quaggin S ,Ghaffari R, Rogersb J A. Passive sweat collection and colorimetric analysis of biomarkers relevant to kidney disorders using a soft microfluidic system. *Lab Chip*. 2019; 19(9): 1545–1555. doi: 10.1039/c9lc00103d
39. Li S, Ma Z, Cao Z, Pan L, Shi Y. Advanced Wearable Microfluidic Sensors for Healthcare Monitoring. *Nano-micro small.* 2020; 16(9) doi: 10.1002/smll.201903822
40. Woodson H. W, Hier S.W, Solomon J.D, Bergeim O. Urinary excretion of amino acids by human subjects on normal diets. *J Biol Chem.* 1948;172(2):613-618. doi:10.1016/S0021- 9258(19)52748-X
41. Hadorn B, Hanimann F, Anders P, Curtius H.C, Halverson R. Free Amino-acids in Human Sweat from Different Parts of the Body. *Nature*. 1967; 215(5099):416–417. doi: 10.1038/215416A0
42. Dunstan R. H, Sparkes D. L,Dascombe B. J,Stevens C. J, Murphy G. R, Macdonald M.M, Gottfries J, Gottfries C.G, Roberts T. K. Sex differences in amino acids lost via sweating could lead to differential susceptibilities to disturbances in nitrogen balance and collagen turnover. *Amino Acids*. 2017; 49**:**1337–1345. doi: 10.1007/s00726-017-2431-4
43. Kalasin S, Sangnuang P, Surareungchai W. Satellite-Based Sensor for Environmental Heat-Stress Sweat Creatinine Monitoring: The Remote Artificial Intelligence-Assisted Epidermal Wearable Sensing for Health Evaluation. *ACS Biomater. Sci. Eng.* 2021; 7(1):322–334 doi: 10.1021/ACSBIOMATERIALS.0C01459/SUPPL_FILE/AB0C01459_SI_002.MP4